http://dx.doi.org/10.1016/j.conbuildmat.2017.05.050

A New and Simplified Approach to Assess the Pavement Surface micro- and macrotexture

Filippo G. Praticò[a], Armando Astolfi[b]

[a]*DIIES Department, University Mediterranea of Reggio Calabria*

[b]*DICAM Department, University of Palermo*

ABSTRACT

Road safety depends on pavement skid resistance and surface texture. Skid resistance mainly depends on micro-texture and macrotexture. Skid and texture measurements on samples, in the laboratory, at the preliminary stage of the design, would enhance the design in terms of timing, costs, and reliability. Consequently, this study aims at setting up and validating simple methods for assessing surface texture and skid resistance based on core/sample measurements. Experiments were carried out and predictive relationships were set up to explain and predict results. Under given conditions, miniaturised macro-and microtexture tests (modified EN 13036-1 and modified EN 13036-4, respectively) prove to be a reliable tool to optimise texture design. Results highlight the suitability of the proposed methodology and can benefit both researchers and practitioners.

Keywords: Pavement Surface Properties, Road Safety, Macrotexture, Micro-texture.

Graphical abstract

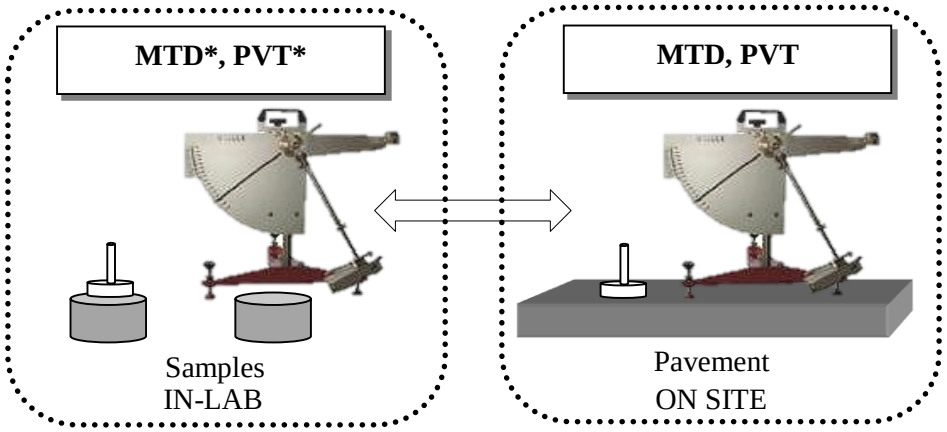

Symbols. MTD: mean texture depth; MTD*: miniaturized mean texture depth; PTV: Pendulum Test Value; PTV*: miniaturized Pendulum Test Value.

1. Introduction

Pavement texture is a continuum which includes different scales, as a function of the wavelength: micro, macro, mega-texture and unevenness [1], [2], [3], [4]. Micro-texture refers to wavelengths, λ, lower than 0.5 mm and peak-to-peak amplitudes, A, in the range 10−3mm–0.5 mm. Macrotexture refers to λ = 0.5–50 mm and A = 0.1 mm–20 mm.

Macrotexture can be assessed through laser-based methods [5], [6], [7], [8], [9], sand-patch-like methods [10], [11], [12], [13], [14], or other extrinsic methods [15]. Methods above differ based on a number of parameters: the "material-method" used to "fill" the texture (sand, glass beads, or laser), the number of points on the surface investigated (1–10), and the number of diameters measured per point (2–4) [11]. The mean texture depth (MTD, [10]) pertains to the macrotexture domain. It usually ranges from 0.3 mm to 0.7 mm for dense-graded friction courses (DGFC) and from 1 mm to 6 mm for porous asphalt concretes (PA) and it requires a surface diameter that is usually between 50 mm and 300 mm [16].

Micro-texture pertains to the roughness of the surface of the exposed aggregate chips that can be felt by one's fingertips. It interacts with the tire rubber on a molecular scale and provide adhesion (one out of the

two key mechanisms of tire-pavement friction, cf. [17]. Research shows that the evolution of the asperity-peak curvature of micro-texture follows that of the surface friction coefficient [18].

Micro-texture values are indirectly estimated in terms of pendulum test value (termed PTV in the standard EN and termed BPN in ASTM and CNR standards), using low speed friction measurement devices such as the British Portable Tester [19], [20]. PVT values usually have to be greater than 45–65 (based on pavement type and road relevance), with measurements baselines which are about 125 mm [21], [22]. Furthermore, surface texture affects friction, in terms of both macrotexture and micro-texture [23], [24], [25], [26], [19].

Pavement micro- and macrotexture are a vital requirement of a pavement because they impact road safety, [1], [17], [27], [28], [29], [30], [31], [32] and greatly affect the state of play of the transportation infrastructure [33]. It turns out that the design of pavement texture at an early stage, in the laboratory, is crucial because of many reasons: i) concurrent requirements have to be satisfied: volumetric properties [34], "premium" properties [35], variations over time [17], [36], [37], [38], and production requirements [39]; ii) the ability of laboratory specimens to reproduce real pavements may be sometimes controversial (cf. [40], [41], [42]) and methods and studies are needed to link field and laboratory results; iii) laboratory experiments enforce scientific control by testing hypotheses in the artificial and highly controlled setting of a laboratory and imply considerable savings. Unfortunately, MTD and PTV measurements require extended surface areas and this hinders from having MTD and PTV estimates based on laboratory samples.

Understanding and deriving relationships between MTD (/PTV) tests carried out on samples and on real pavements is crucial: 1) to asses if mixes with identical volumetrics and components may have surface properties which are significantly different based on on-site vs. in-lab compaction [43], [44]; 2) given the above, to help carry out a realistic design of surface characteristics during the so-called prequalification of the mix friction course. This research gap calls for research and investigation.

2. Objectives

The main objective of the study described in this paper is to provide a theoretical and practical framework to carry out micro- and macrotexture measurements at the design stage, on samples or small slabs, in the laboratory. In more detail: i) standardized measurements were carried out on several friction courses according to the sand patch method [10] and to the British Pendulum Method [21]; ii) both dense-graded and open-graded friction courses were considered; iii) in-lab and on-site tests were carried out; iv) the tests were both modelled. Algorithms were set up and finally applied to explain results and predict further developments. This paper illustrates the results obtained in terms of miniaturization of macrotexture measurements and micro-texture measurements. Section 3 refers to experiments while a Section 4 focuses on modelling, calibration, and validation. Finally, in Section 5, conclusion are drawn and main contributions are pointed out.

3. Experiments

In task 1, in the aim of gathering practical information and data about the potential of the two tests to be used in the laboratory, experiments were carried out on pavements and on cores extracted. Six reference friction courses were considered: three dense-graded friction courses (DGFC), herein termed DG1-DG3, and three porous asphalt concretes (PA), herein termed PA1-PA3. On average, for DGFCs, specific gravity was 2.32 and asphalt binder content was 5.1% (by weight of mix), while for PAs, specific gravity was 2.11 and asphalt binder content was 5.0% (by weight of mix). Two types of indicators were derived: Mean Texture Depth (MTD, [10]) and Pendulum Test Value (PVT, [21]). The volume used to measure MTD and the length of the contact path were the ones set up in the concerned standards (UNI EN 13036-1 [10] and UNI EN 13036-4 [21]) and the ones needed in order to make it possible to perform them on samples, in the laboratory.

3.1. Macrotexture

For macrotexture, note that a volume of 25,000 mm3 is required by the traditional, current methods [1], [11], [12], while a smaller volume (4500 mm3, [45]) is required by the diameter of Marshall [46] or gyratory specimens [47]. By referring to the miniaturization of the MTD test, it appears relevant to observe that when sample, sand patch, and spreading tool are considered: the sample diameter varies from “infinity”

(pavement), to about 100 mm (Marshall specimen), while the spreading tool has a constant diameter of 63.5 mm, and the sand patch diameter varies based on mix type, compaction and volume.

In each point of each surface (e.g., point B of surface DG1), multiple repetitions of the MTD measurement were carried-out (up to 31, Table 1). For V = 4500 mm3, note that each measurement was followed by compressed air jet blasting in order to clean the surface and that this procedure is not usually required because both CNR and EN-ASTM standards do not require to repeat the measurement in the same point of the surface. Table 1 illustrates the averages obtained for the six pavements under analysis. Values in the range 0.5 mm–1.9 mm were obtained for DGFCs. On the contrary, values between 1.6 mm and 2.9 mm were obtained for PAs. Note that the standard deviation ranged from 0.01 mm to 0.22 mm for DGFCs, while it ranged from 0.00 mm to 0.10 mm for PAs. Note that DG1 differs from DG2 and DG3 and this may be due to the fact that DG1 corresponds to a dense-grade friction course that is older than DG2 and DG3. This partly complies with Iuele [43] and Do [48] and refers to the fact that surface texture deterioration is greater than for the other two types of surface. Many factors, including aggregate properties, binder properties, aggregate-binder combination, road geometry, traffic, weather, rainfall, and environmental conditions can be responsible for this [43], [48], [49], [50], [51], [52]. Table 1 also illustrates the coefficients of variation (CV, ratio of standard deviation to mean) for each mix (with V = 4500 mm3 and V = 25,000 mm3). DGFCs have CVs lower than 14%, while PAs have CVs lower than 4%. It is possible to observe that:

- the higher the volume is, the higher the MTD becomes;
- the standard deviation decreases when the volume used increases from 4500 mm3 to 25,000 mm3;
- the coefficient of variation (CV) decreases when the volume increases;

RMTD is the ratio MTD25/MTD4.5, i.e., the ratio between the value of MTD obtained when using a volume of 25,000 mm3 or 4500 mm3. By referring to RMTD = MTD25/MTD4.5 (Table 1), note that this ratio ranges from 103% to 121% for the dense-graded friction courses considered, while it ranges from 102% to 123% for porous asphalt concretes.

It is noted that high values of MTD (e.g. PA2) may be linked to sand percolation into the interconnected pores “under the surface”, which may imply higher variances for MTD and RMTD and non-linearities in MPD-MTD relationship [53].

Table 1: MTD values obtained according to the UNI EN 13036-1 [**Errore. L'origine riferimento non è stata trovata.**]

Sample	DG1		DG2		DG3		PA1		PA2		PA3	
V	25000	4500	25000	4500	25000	4500	25000	4500	25000	4500	25000	4500
MTD	1.90	1.57	0.50	0.46	0.50	0.48	2.02	1.64	2.89	2.83	1.76	1.60
R_{MTD}	-	1.21	-	1.09	-	1.03	-	1.23	-	1.02	-	1.10
$1/R_{MTD}$	-	0.83	-	0.91	-	0.97	-	0.81	-	0.98	-	0.91
S.D.	0.06	0.22	0.01	0.03	0.01	0.03	0.06	0.03	0.00	0.10	0.05	0.07
CV	3%	14%	2%	6%	2%	7%	3%	2%	0%	4%	3%	4%

Symbols. V: Volume of sand [mm^3]; MTD: Mean Texture Depth, mm [**Errore. L'origine riferimento non è stata trovata.**]; R_{MTD}: ratio $MTD_{25}/MTD_{4.5}$; MTD_{25}: Mean Texture Depth corresponding to V=25000 mm^3; $MTD_{4.5}$: Mean Texture Depth corresponding to V=4500 mm^3; S.D.: Standard Deviation [mm]; CV: Coefficient of Variation [%]; DG1-DG3: dense-graded friction courses; PA1-PA3: porous asphalt concretes.

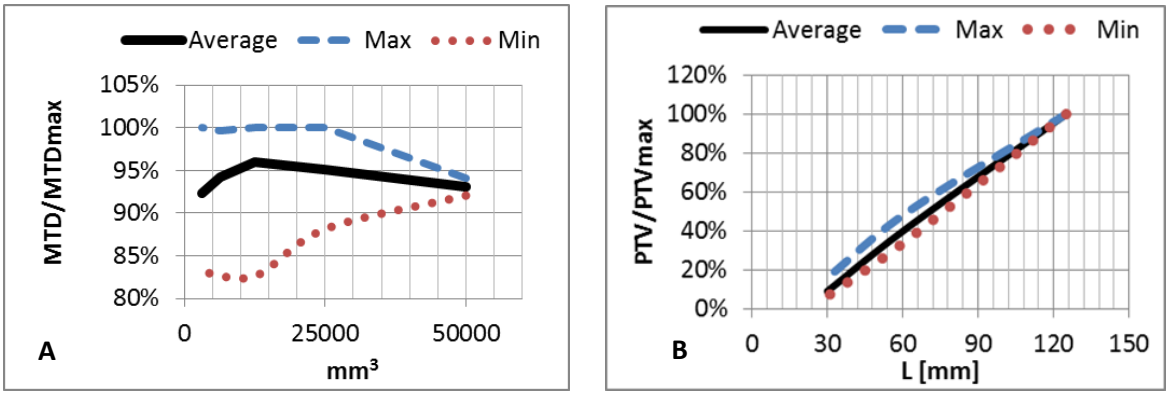

Figure 1: Preliminary tests performed (example: left/A: MTD as a percentage of the maximum value; right/B: PTV).

4.2 Skid resistance

For skid resistance, preliminary tests were carried out in order to explore for different slide lengths (cf. Fig. 1B). For both PTV and MTD, note that the smaller the lengths/surfaces are, the higher the variability is. Table 2 refers the results (PTV) obtained for dense-graded mixtures (DG1-DG3) and porous asphalt concretes (PA1-PA3), when using the slide length as per standard (L = 125 mm) or reducing it in the pursuit of miniaturization (L = 62.5 mm).

Each result (e.g., PTV = 76) refers to a given sample and is the average of 6 values. In turn, each of these six values is the average of 5 "swings". In summarising, each results derives from 30 "swings". The coefficient of variation (CV,%) is derived starting from the standard deviation and the average (PTV).

1/R refers to the ratio PTV62.5/PTV125 (same mixture, e.g., DG2). Note that PTV125/PTV62.5 ranges from 1.99 to 2.77 (all the samples) and its average is 2.40. In contrast, PTV125/PTV62.5 ranges from 1.99 to 2.22

and its average is 2.14 for porous concretes (PAs), while PTV125/PTV62.5 ranges from 2.48 to 2.77 and its average is 2.66 for dense-graded friction courses (DGs).

Note that: i) PTV ranges from 59 to 76 for DGs and from 59 to 61 for PAs (L = 125 mm); ii) If the contact path is halved then the results obtained decrease and the standard deviation increase; iii) RPVT ranges from 1.9 to 2.2 for DGs and from 2.4 to 2.7 for Pas; iv) 1/RPTV ranges from 36 to 50%.

Table 2: PTV values obtained according to UNI EN 13036-4 [**Errore. L'origine riferimento non è stata trovata.**]

Sample	DG1		DG2		DG3		PA1		PA2		PA3	
L	125.0	62.5	125.0	62.5	125.0	62.5	125.0	62.5	125.0	62.5	125.0	62.5
PTV	76	34	59	29	64	29	59	21	59	24	61	22
CFT	-3	-2	-2	-2	-2	-2	-2	-2	-2	-2	-2	-2
R_{PVT}	-	2.20	-	1.99	-	2.22	-	2.77	-	2.48	-	2.74
$1/R_{PVT}$	-	0.45	-	0.50	-	0.45	-	0.36	-	0.40	-	0.37
S.D.	1.53	1.11	1.09	1.23	1.00	0.72	1.27	1.16	1.12	0.84	2.06	0.76
CV	2%	3%	2%	4%	2%	2%	2%	5%	2%	3%	3%	3%

Symbols. L: Slide length [mm]; PTV: Pendulum Test Value [**Errore. L'origine riferimento non è stata trovata.**]; R_{PVT}: ratio $PTV_{125}/PTV_{62.5}$; PTV_{125}: Pendulum Test Value corresponding to L=125 mm; $PTV_{62.5}$: Pendulum Test Value corresponding to L=62.5 mm; S.D.: Standard Deviation; CV: Coefficient of Variation [%]; DG1-DG3: dense-graded friction courses; PA1-PA3: porous asphalt concretes; CFT correction factor for temperature.

4. Modelling, calibration, and validation

In order to explain the rationale behind the results obtained, attention was focused on modelling both tests. In both cases, analyses were carried out to simulate what happens when small surfaces are used, in the aim of providing insights and explanations.

4.1. MTD modelling

As is well known, MTD is the ratio between a given volume, V (e.g. V_{25}= 25000 mm^3 or $V_{4.5}$= 4500 mm^3), and the corresponding area ($\pi D^2_{25}/4$ or $\pi D^2_{4.5}/4$, respectively):

$$MTD = \frac{4 \cdot V}{\pi \cdot D^2} \quad \text{(Eq. 1)}$$

Where D (e.g., D_{25}) is the diameter of sand patch. If R is the ratio between MTD_{25} (volume=25000 mm^3) and $MTD_{4.5}$ (volume=4500 mm^3), for the diameters of sand patch, $D_{4.5}$ and D_{25}, it follows:

149 $$\frac{D_{25}^2}{25} = \frac{1}{R}\frac{D_{4.5}^2}{4.5} \quad \text{(Eq. 2)}$$

150 Under the hypothesis that R>1, it follows:

151 $$\frac{D_{25}^2}{25} < \frac{D_{4.5}^2}{4.5} \quad \text{(Eq. 3)}$$

152 By referring to the reasons for having such a relationship (as observed in the experiments), different
153 hypotheses might be formulated, among which the following: i) Results are affected by spreading procedure
154 and by the ratio DST/DV, where DST is the diameter of the spreading tool (63.5 mm), while DV is the
155 diameter of the sand patch for the given volume (V); ii) when smaller quantities of sands are investigated, for
156 the relationship between MTD (dependent variable) and the volume of sand used (V, independent variable),
157 there are local domains of V in which the first derivative changes sign.
158 In order to provide explanations, let us model surface texture in terms of spherical holes on a flat surface (see
159 Fig. 2).

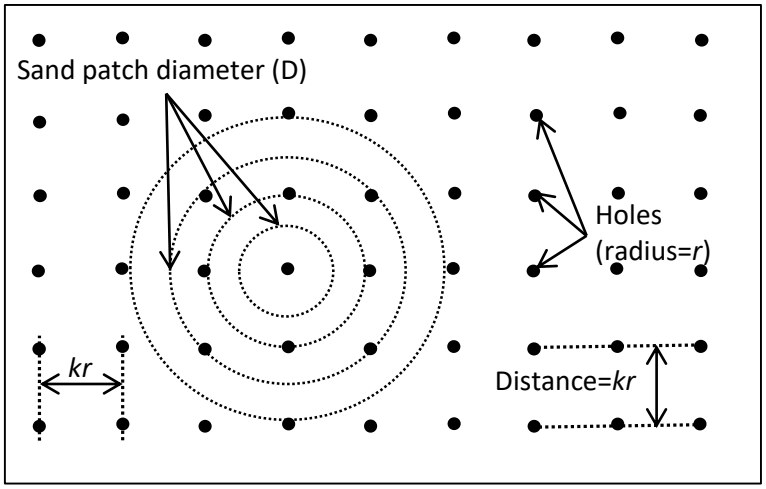

160

161 **Figure 2:** Modelling sand patch test in an ideal surface.

162 Let us suppose that the volume of each hole is:

163 $$V_H = \frac{2\pi \cdot r^3}{3} \quad \text{(Eq. 4)}$$

164 Where V_H (mm^3) is the volume of the given hole and r (mm) is the radius of the semi-sphere. Let us suppose
165 that the distance (centre to centre) between two adjacent spheres is $k \cdot r$ on both the x-axis and the y-axis
166 (k≥2). For D>>2r, the number of semi-spheres is approximately given by:

$$N \cong \left(\frac{(D - 2 \cdot r)}{k \cdot r \cdot \sqrt{2}} + 1 \right)^2 \quad \text{(Eq. 5)}$$

Consequently it results approximately that:

$$\text{for } \frac{(D - 2 \cdot r)}{k \cdot r \cdot \sqrt{2}} \geq 1 \qquad MTD \cong \left[\frac{(D - 2 \cdot r)}{k \cdot r \cdot \sqrt{2}} + 1 \right]^2 \cdot \frac{\frac{2}{3} \pi \cdot r^3}{\frac{\pi D^2}{4}} + 0.2 \ \text{[mm]} \quad \text{(Eq. 6)}$$

and

$$\text{for } \frac{(D - 2 \cdot r)}{k \cdot r \cdot \sqrt{2}} < 1 \qquad MTD \cong 0.2 \ \text{[mm]} \quad \text{(Eq. 7)}$$

when D approaches infinity, then it results:

$$\lim_{D \to \infty} (MTD) \cong \frac{4 \cdot r}{3k^2} + 0.2 \quad \text{(Eq. 8)}$$

Based on the algorithms herein set up (Eqs. (5), (6), (7), (8)) it follows that:

- The lowest value depends on sand diameter (0.2 mm);
- The highest value depends on hole geometry;
- The higher D becomes, the lower the variability of MTD is (cf. Fig. 3-A). The asymptotic value depends on the geometric model.

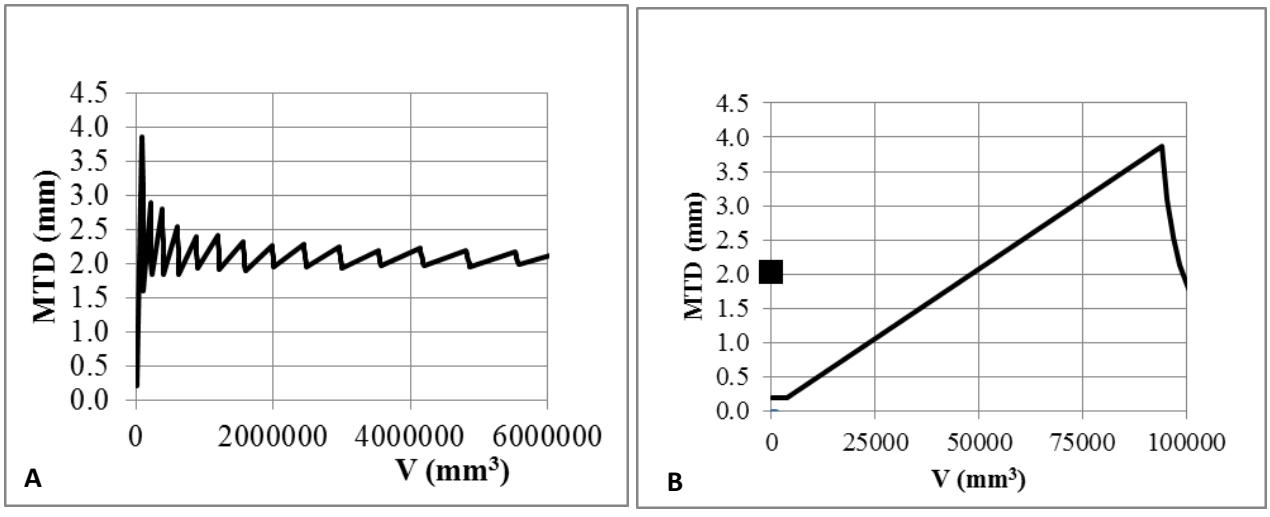

Figure 3: MTD predicted through the model.

The rationale behind Eq. (6) is that MTD is given by 0.2 mm (i.e., sand diameter) plus 1, 9, 25 times the volume of a semisphere divided by the overall surface area covered. The multiplier is in square brackets.

Fig. 3 refers to how MTD (y-axis, Eq. (6)) varies based on the volume of sand (x-axis). It appears evident that the model confirms that there are contexts in which the first derivative may be positive and, vice versa, there are situations in which the first derivative may be negative.

Model predictions (see Fig. 3) confirm that the first derivative undergoes different values (positive and negative), due to the fact that sand can be spread over sags, crests, or flat surfaces.

For the number of repetitions, note that based on the dependence of the standard deviation of the mean (SDOM) on the number of repetitions, for a volume of 4500 mm3, 4 repetitions are needed in order to have a standard deviation-to-average ratio of 2% (as per EN and ASTM standards).

Table 3 summarises the main characteristics of the proposed method for the miniaturization of MTD test.

By referring to test repeatability and reproducibility (CV% s.o. and CV% d.o., respectively, cf. Table 3), it appears noteworthy to highlight that in ASTM E 965 [11] and UNI EN 13036-1 [10] it is reported that "The standard deviation of the site-to-site measurements may be as large as 27% of the average texture depth", where site "defines a randomly selected location within a nominally homogeneous pavement section". In contrast, fixed-site CV is about 1–2%.

Table 3: Characteristics of the proposed method.

Standard	CNR BU 94/83	UNI EN 13036-1	ASTM E 965	Proposed
Points	5 + 5	4	4	1
Diameters	2	2	2	2
Distribution	2A	Random	Random	COS
CV% s.o.	N.A.	1% (*)	1% (*)	2%
CV% d.o.	N.A.	2% (*)	2% (*)	2%
Repetitions	1	1	1	4
Cleaning	N.A.	N.A.	N.A.	CA

Symbols. (*): Macrotexture depth of 0.5 to 1.2 mm; N.A.: not available; s.o.: same operator; d.o.: different operator; Points: number of points for the given surface; Diameters: number of diameters per point; Distribution: distribution of points on the surface; CV%: Precision in terms of coefficient of variation in percentage; Repetitions: number of repetitions in the same point; 2A: two alignments (quasi-deterministic); CV%: coefficient of variation in percentage. CA: compressed air. COS: centre of specimen [**Errore. L'origine riferimento non è stata trovata.**].

4.2. PTV modelling

As is well known, following da Vinci observations, Amontons' laws states that the ratio of the friction force to the loading force (friction coefficient) does not depend on the loading force or the apparent contact area.

When an object begins to slide, it is often considered that a shear force greater than the maximum static friction force is needed. This notwithstanding, according to Otsuki & Matsukawa [54], precursors appear as local slips at the interface under shear forces quite below before the maximum static friction force, and this force corresponds to the onset of bulk sliding. According to Tuononen [55], the onset of the frictional sliding (i.e., when the phenomenon commences) depends on the state of the surfaces between the two sliding materials. In more detail, Tuononen [55] focuses on rubber–glass contact under dry and lubricated conditions and obtained different curves. For rubber on dry glass, the force curve over time undergoes a smooth transition from the static situation (friction coefficient zero) to sliding (friction coefficient quasi-constant), without any identifiable peak value, and with no precursors of sliding. For rubber on wet glass, the force curve over time shows a clear peak value (which would traditionally be the static friction coefficient), involved phenomena are more complex, and after the peak a quasi-constant value is approached (over time).

Based on theory and based on preliminary experiments, an equation in which the sliding force varies over space according to a three-step model is formulated in this paper. In order to derive information about the expected variation of PTV when different lengths of contact path are considered, let us consider that the pendulum motion starts from a given height (h1) and ends at a given height (hF), due to two main classes of energy losses (Fig. 4): i) friction losses (W) in the contact path between pavement/core and the pendulum rubber shoe (slider assembly), based on friction coefficient (μ), on reference orthogonal force (Fort) and on contact length ($L = A + B + (L - A - B)$); ii) friction losses in the hinge of the device, which refer to hpiv (see below) and $h*$ (zero reading below the horizontal, [56], [57], [58]).

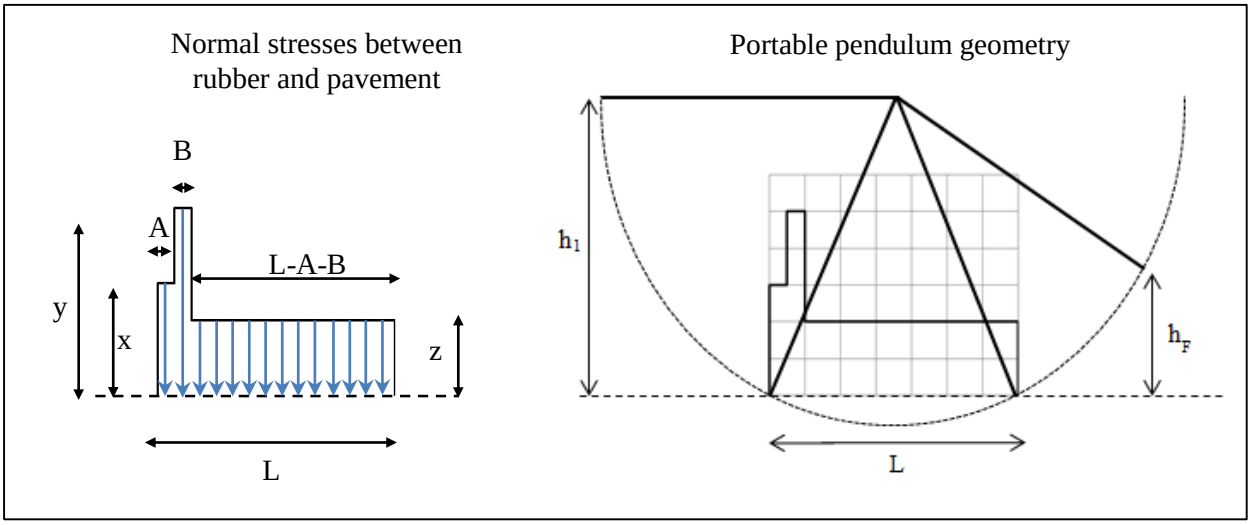

Figure 4: PTV stress distribution (left) and test geometry (right)

The main algorithms herein set up are summarised in Eqs (9), (10), (11), (12), (13), (14).

The relationship between PTV_{ob125} (PTV observed, L=125 mm) and the friction coefficient is as follows:

$$\mu = \frac{PTV_{ob12.5}}{100} \qquad \text{(Eq. 9)}$$

Three stretches (A, B, L-A-B) in the contact path L are supposed to exist, with a contact force which undergoes corresponding changes (x F_{ort} in A, y F_{ort} in B, z F_{ort} afterwards):

$$W = F_{ort} \cdot \mu \cdot \left[Ax + By + (L - A - B)z\right] \qquad \text{(Eq. 10)}$$

The final height (no friction at hinge) is as follows:

$$h_2 = \frac{1}{mg}\left[(\frac{1}{2}m \cdot 2h_1 \cdot g) - W\right] \qquad \text{(Eq. 11)}$$

where m≅ 1.5±0.03 kg [**Errore. L'origine riferimento non è stata trovata.**], g= 9.81m/s^2, h_1≈ 0.512m, F_{ort}≈ 22.5N.

The final height results:

$$h_F = h_2 - h_{piv} = h_2 - \frac{h_2}{h_1}h^* \qquad \text{(Eq. 12)}$$

where h^*= 0.01016m.

Based on the as-built characteristics of the British Pendulum, the relationship between the final height (h_F) and the value of PTV is here estimated as follows:

242 $$PTV_e = -0.7013 \cdot h_F + 352.06$$ (Eq. 13)

243 Overall, based on tests, the calibration of the proposed model is carried out through the following error
244 function (objective function):

245 $$\Phi = \sum (PTV_e - PTV_{ob})^2$$ (Eq. 14)

246 where PTV_{ob} is the value observed, while PTV_e is the value estimated through the equation above.

247 ### *4.3. Calibration and validation*

248 PTV model calibration was carried out based on equations above. Based on results it is possible to observe
249 that, for the cases under analysis: i) on average there are three different steps/phases in rubber vs. pavement
250 sliding. In the first phase (length A < 15 mm) there is a force which is less than 1% of the reference force set
251 up un the standard (22.5 N). In the second phase (length B < 0.3 mm), there may be an increase of the
252 reciprocal, orthogonal force. This supplementary phase (B), if existing, accounts for less than 1 cm of sliding
253 path. In the third phase (L-A-B), which corresponds to almost the entire sliding length (L), the force is close
254 to 100% of the reference force; ii) overall an average error of 1–3 PTV points was obtained, as a function of
255 the minimization process chosen; iii) Fort resulted to range from 17 to 23 N; iv) in all the optimizations
256 attempts, PTV62.5/PTV125 resulted close to 44%.

257

258 In summarising, based on modelling it appears that the results obtained and the relationship between contact
259 length and results are well explained by the physical model set up herein.

260

261 By referring to the number of repetitions and to the precision of the proposed and miniaturised method (see
262 Table 4), note that: i) the EN 13036-4 [21] states that the precision is 1 PTV, uncorrected for temperature and
263 on a fine-textured, plane surface. At the same time, it mentions that coarse textured or very smooth surfaces
264 will reduce the precision and it warns about porous surfaces on which the test may give erroneous results.
265 Furthermore, the same standard states that (Note 2) the use of the temperature correction will reduce the

precision of the test and that (10.3) the number of samples necessary to obtain the PTV of an area will be dependent upon the variability of the surface; ii) experiments prove that the miniaturised method has a standard deviation which is close to 1 PTV (0.7 for the tests under investigation); iii) the EN precision in terms of standard deviation corresponds to a precision in terms of coefficient of variation of about 1.6%; iv) based on the above, it is suggested to perform at least six tests (each test consisting of five swings) for dense-graded friction courses and at least nine tests (each test consisting of five swings) for porous asphalt concretes. These repetitions (e.g., 1·6·5 for DGFCs) make the standard deviation of the miniaturised test consistent with the one of the EN standard for both DGFCs and PAs.

Based on the above, Table 4 summarises the characteristics of the proposed method.

Table 4: Characteristics of the proposed method (PTV-BPN).

Standard	ASTM E 303	UNI EN 13036-4	CNR 105/85	Proposed
Points	4-5	≥3	5·3	1
Measures *per* point	1	1	1	6-9 (*)
Swings *per* point	>4	5	5	5
Distribution of points	N.A.	Random	3A	COS
S.D.	1-1.2 BPN unit	1 PTV	1.2 BPN unit	1 PTV

Symbols. 3A: three alignments (quasi-deterministic) in areas more stressed by traffic; COS: centre of specimen; S.D.: Standard Deviation; N.A.: not available; (*): 6·5 swings for DGFCs, 9·5 swings for PAs.

Figure 5 summarizes model validation. Validation data were independently measured from the calibration data.

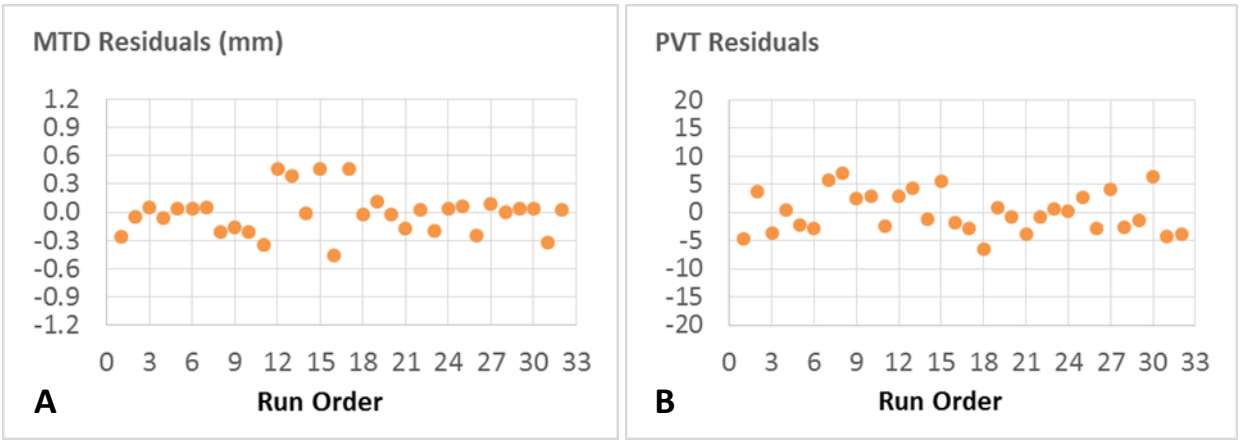

Figure 5: Run sequence plot for the residuals (MTD: Fig.5A; PTV: Fig.5B).

Fig. 5A (left) focuses on MTD. Note that R-square is 0.93 while the residual scatter plot shows no systematic patterns apparent. This indicates that the model fits the data well. Fig. 5B (right) refers to PVT. This plot shows that there is only random scatter in the relationship between the observed PTV and the order in which the data were collected. Note that in this case the R-square is only 0.4. This fact may be due to the high standard deviation of PAs and calls for further study and research.

5. Conclusions and contribution

Based on the results shown above it may be observed that for macrotexture:

4500 mm3 are appropriate for Marshall/Giratory specimens and for different types of mixes, included DGFCs and PAs;

The miniaturised MTD (V = 4500 mm3) is approximately 10% less than the one obtained according to in-situ tests (for both PAs and DGFCs). This implies that the results should be consequently corrected (R = 1.02–1.23);

Four measurements are needed in order to have a σ/MTD ratio complying with the one stated in the ASTM-EN standards;

Due to the small quantity of sand and to the complexity of surface texture, modelling explains that MTD measurements are affected by the volume of sand used.

At the same time, for skid resistance:

- A contact path of 62.5 mm is appropriate for Marshall/Giratory specimens of different types of mixes, including DGFCs and PAs;
- The value of PTV which is obtained when using a length of 62.5 mm is approximately 58% less than the one obtained according to in-situ tests (for both PAs and DGFCs). This implies that the results should be consequently corrected (R = 1.99–2.77);
- Based on the dispersion indicators obtained, 6–9 measures per point are needed in order to have a precision complying with the one stated in the ASTM E 303 [59] and in the EN 13036-4 [21];
- Test model set up and calibrated explains that lower contact paths correspond to lower PTVs and quantifies the difference with a fair precision (44% versus 42%, on average).

Based on the above, it seems possible to point out that this paper makes several contributions to the literature. First, this study adds to the relatively small amount of research that examines whether macrotexture and pendulum test can be explained and predicted based on simple physical and geometric models.

Second, the results of this study help provide a better understanding of the importance and the criticalities of assessing macro- and micro-texture at an early stage and on small samples.

Whereas previous research provides evidence that small samples may provide valuable information about texture, this study reveals that such measures can be related to the corresponding measures on real pavements.

Finally, evidence of methods to limit the uncertainties in texture prediction may be of interest to practitioners and researchers.

6. References

[1] M.B. Snyder, Current Perspectives on Pavement Surface Characteristics, ACPA publication EB235P Pavement Surface Characteristics: A Synthesis and Guide. R&T Update, Concrete Pavement Research & Technology, Number 8.02, 2007.

[2] Chengyi Huang, Shunqi Mei, Investigation of Road Surface Texture Wavelengths, New Tribological Ways, Dr. Taher Ghrib (Ed.), ISBN: 978-953-307-206-7, 2011.

[3] L.G. Andersen, J.K. Larsen, E.S. Fraser, B. Schmidt, J.C. Dyre
Rolling resistance measurement and model development
J. Transp. Eng., 141 (2) (2015), p. 04014075

[4] A. Dunford
Friction and the Texture of Aggregate Particles Used in the Road Surface Course
(Ph.D thesis)
University of Nottingham, UK (2013)

[5] E. Astm
Standard Practice for Calculating Pavement Macrotexture Mean Profile Depth

ASTM International, West Conshohocken, PA (1845), p. 2015

[6] ISO 13473-1, Characterization of Pavement Texture by use of Surface Profiles. Part 1: Determination of Mean Profile Depth, 2013.

[7] ASTM E 2157

Standard Test Method for Measuring Pavement Macrotexture Properties Using the Circular Track Meter

ASTM International, West Conshohocken, PA (2015)

[8] ISO 13473-2

Characterization of Pavement Texture by Use of Sur-face Profiles – Part 2: Terminology and Basic Requirements Related to Pavement Texture Profile Analysis

(2002)

[9] ISO 13473-3

Characterization of Pavement Texture by Use of Sur-face Profiles. Part3: Specifications and Classification Of Profilometers

(2002)

[10] UNI EN 13036-1

Road and Airfield Surface Characteristics - Test Methods - Part 1: Measurement of Pavement Surface Macrotexture Depth Using a Volumetric Patch Technique

Ente Nazionale Italiano di Unificazione, Milano, Italia (2010)

[11] ASTM E 965

Standard Test Method for Measuring Pavement Macrotexture Depth Using a Volumetric Technique

ASTM International, 100 Barr Harbor Drive, PO Box C700, West Conshohocken, PA 19428-2959, United States (2006)

[12] CNR B.U. 94/1983, Norme per la misura delle caratteristiche superficiali delle pavimentazioni – Metodo di prova per la misura della macro-rugosità superficiale con il sistema della altezza di sabbia, Consiglio Nazionale delle Ricerche Anno XVII, pt. IV, n.94 (1983), pp. 3–20.

[13] Colorado Procedure 77-09, Determination of Macro-Texture of Planed Hot Mix Asphalt Pavement, 2009.

[14] Colorado Procedure 77-14, Determination of Macro-Texture of a Pavement Surface, 2014.

364 [15] ASTM E 2380/E 2380M
365 Standard Test Method for Measuring Pavement Texture Drainage Using an Outflow Meter
366 ASTM International, West Conshohocken, PA (2015)
367 [16] ANAS, Capitolato Speciale d'Appalto – Parte 2a Norme Tecniche Pavimentazioni
368 stradali/autostradali, Ministero delle Infrastrutture e dei Trasporti – Ispettorato per la Circolazione e la
369 Sicurezza Stradale – CIRS, Centro Sperimentale Interuniversitario di Ricerca Stradale, 2009.
370 [17] R.B. Kogbara, E.A. Masada, E. Kassem, A. Scarpas, K. Anupam
371 A state-of-the-art review of parameters influencing measurement and modeling of skid resistance of
372 asphalt pavements
373 Constr. Build. Mater., 114 (1) (July 2016), pp. 602-617
374 [18] A.D. Nataadmadja, M.T. Do, D.J. Wilson, S.B. Costello, Quantifying aggregate microtexture with
375 respect to wear—Case of New Zealand aggregates, Wear, Volumes 332–333, May–June 2015, pp. 907–
376 917.
377 [19] J.N. Meegoda, S. Gao
378 Evaluation of pavement skid resistance using high speed texture measurement
379 J. Traffic Transp. Eng. (English Edition), 2 (6) (2015), pp. 382-390
380 [20] J.C. Wambold, J.J. Henry
381 International PIARC experiment to compare and harmonize texture and skid resistance measurements
382 Nordic Road Transp. Res., 6 (2) (1995), pp. 28-31
383 [21] UNI EN 13036-4, Road and airfield surface characteristics – Test methods – Part 4: Method for
384 measurement of slip/skid resistance of a surface: The pendulum test, 2011.
385 [22] CNR B.U. 105/1985, Norme per la misura delle caratteristiche superficiali delle pavimentazioni -
386 Metodo di prova per la misura della resistenza di attrito radente con l'apparecchio portatile a pendolo,
387 1985.
388 [23] G.G. Balmer
389 Pavement texture: its significance and development
390 Transp. Res. Board Res. Rec., 666 (1979), pp. 1-6
391 [24] M. Ergun, S. Lyinam, A.F. Lyinam

392 Prediction of road surface friction coefficient using only macro- and micro-texture measurements
393 J. Transp. Eng., 131 (4) (2005), pp. 311-319
394 [25] N.M. Jackson, B. Choubane, C.R. Holzschuher
395 Measuring Pavement Friction Characteristics at Variable Speeds for Added Safety Pavement Surface
396 Condition/Performance Assessment: Reliability and Relevancy of Procedures and Technologies
397 ASTM, West Conshohocken (2007)
398 STP 1486
399 [26] M.A. Khasawneh, R.Y. Liang, Correlation study between locked-wheel skid trailer and dynamic
400 friction tester, TRB 87th Annual Meeting, Washington DC, 2008.
401 [27] D. Woodward, P. Millar, C. Lantieri, C. Sangiorgi, V. Vignali
402 The wear of Stone Mastic Asphalt due to slow speed high stress simulated laboratory trafficking
403 Constr. Build. Mater., 110 (2016), pp. 270-277
404 [28] V.M.C. Araujo, I.S. Bessa, V.T.F. Casteli Branco
405 Measuring skid resistance of hot mix asphalt using the aggregate image measurement system (AIMS)
406 Constr. Build. Mater., 98 (2015), pp. 476-481
407 [29] D.A. Noyce, H.U. Bahia, J.M. Yambò, G. Kim, Incorporating road safety into pavement
408 management: Maximizing asphalt pavement surface friction for road safety improvements, Draft
409 Literature Review & State Surveys, Midwest Regional University transportation Center Traffic
410 Operations and Safety (TOPS) Laboratory, 2005.
411 [30] U. Sandberg, Influence of road surface texture on traffic characteristics related to environment,
412 economy and safety: A state-of-the-art study regarding measures and measuring methods, Swedish
413 National Road and Transport Research Institute. Road Maintenance and Operation, Project n. 20229,
414 Measurement of road surface texture, Swedish, 1998.
415 [31] F.R. Zhao, T.J. Qiu, H. Zhang
416 Effect of macro-texture features on anti-sliding characteristics of cement concrete pavement
417 Zhongguo Gonglu Xuebao/China J. Highway Transport, 29 (7) (2016), pp. 15-21
418 [32] L.J. Chu, T.F. Fwa, K.H. Tan
419 Considering Aggregate Polishing Effect in Prediction of Pavement Skid Resistance

Proc. of the Eighth Intl. Conf. on Maintenance and Rehabilitation of Pavements, Research Publishing, Singapore (2016), 10.3850/978-981-11-0449-7-238-cd
ISBN: 978-981-11-0449-7
[33] M.N. Postorino, F.G. Praticò
An application of the multi-criteria decision-making analysis to a regional multi-airport system
Res. Transp. Bus. Manage., 4 (2012), pp. 44-52
[34] F.G. Praticò, A. Moro
In-lab and on-site measurements of hot mix asphalt density: convergence and divergence hypotheses
Constr. Build. Mater., 25 (2) (2011), pp. 1065-1071
[35] K.P. Biligiri
Tyre/road noise damping characteristics using nomographs and fundamental vibroacoustical relationships
Transp. Res. Part D: Transp. Environ. (2016)
[36] F.G. Praticò, R. Ammendola, A. Moro
Factors affecting the environmental impact of pavement wear
Transp. Res. Part D: Transp. Environ., 15 (3) (2010), pp. 127-133, 10.1016/j.trd
ISSN 1361–9209
ArticleDownload PDFView Record in ScopusGoogle Scholar
[37] F.G. Praticò, R. Vaiana
Improving infrastructure sustainability in suburban and urban areas: is Porous asphalt the right answer? And how?
C.A. Brebbia, J.W.S. Longhurst (Eds.), Urban Transport: Urban Transport and the Environment in the 21st Century, WIT Transactions on Ecology and the Environment, WIT Press (2012), pp. 673-684
ISBN: 9781845645809
[38] F.G. Praticò, A. Casciano
Variability of HMA characteristics and its influence on pay adjustment
J. Civil Eng. Manage., 21 (1) (2015), pp. 119-130
[39] F.G. Praticò

448 Metrics for management of asphalt plant sustainability
449 J. Constr. Eng. Manage. (2017), 10.1061/(ASCE)CO.1943-7862. 00012
450 [40] P. Georgiou, A. Loizos
451 A laboratory compaction approach to characterize asphalt pavement surface friction performance
452 Wear, 311 (2014), pp. 114-122
453 [41] S.N. Goodman, Y. Hassan, A.O. AbdElHalim
454 Preliminary estimation of asphalt pavement frictional properties from Superpave gyratory specimen and
455 mix parameters
456 Transp. Res. Rec., 2006 (1949), pp. 173-180
457 [42] G. Boscaino, B. Celauro, C. Celauro, A. Amadore
458 Evaluation of the laboratory prediction of surface properties of bituminous mixtures
459 Constr. Build. Mater., 23 (2) (2009), pp. 943-952
460 [43] T. Iuele
461 Road surface micro - and macrotexture evolution in relation to asphalt mix composition
462 Hu (Ed.), Advanced Materials and Structural Engineering, Taylor & Francis Group, London (2016)
463 ISBN 978-1-138-02786-2
464 [44] F.G. Praticò, R. Vaiana
465 A study on volumetric versus surface properties of wearing courses
466 Constr. Build. Mater., 38 (2013), pp. 766-775, 10.1016/j.conbuildmat.2012.09.021
467 [45] F.G. Praticò, S. Noto, A. Astolfi, In-lab versus on-site measurement of surface performance of
468 flexible pavements, in: Tenth International Conference on the Bearing Capacity of Roads, Railways and
469 Airfields, 2017.
470 [46] UNI EN 12697-30
471 Bituminous Mixtures – Test Methods for Hot Mix Asphalt – Part 30: Specimen Preparation by Impact
472 Compactor
473 Ente Nazionale Italiano di Unificazione, Milano, Italia (2012)
474 [47] UNI EN 12697-31

475 Bituminous Mixtures - Test Methods for Hot Mix Asphalt - Part 31: Specimen Preparation by Gyratory
476 Compactor
477 Ente Nazionale Italiano di Unificazione, Milano, Italia (2007)
478 [48] M.T. Do, L.P. Kerzreho, J.M. Balay, M. Gothie, Full Scale Tests for the Assessment of Wear of
479 Pavement Surfaces, TRB 82nd Annual Meeting (Transportation Research Board), 2013.
480 [49] S. Li, D. Harris, T. Wells
481 Surface texture and friction characteristics of diamond-ground concrete and asphalt pavements
482 J. Traffic Transp. Eng. (Engl. Ed.), 3 (5) (2016), pp. 475-482
483 [50] R. Vaiana, G.F. Capiluppi, V. Gallelli, T. Iuele, V. Minani
484 Pavement surface performances evolution: an experimental application, SIIV – 5th International
485 Congress – Sustainability of Road Infrastructures
486 Procedia – Social and Behavioral Sciences, 53 (2012), pp. 1151-1162
487 [51] R. Roque, A. Ravanshad, G. Lopp
488 Use of Aggregate Image Measurement System (AIMS) to Evaluate Aggregate Polishing in Friction
489 Surfaces, Florida Department of Transportation Research Management Center
490 University of Florida Department of Civil and Coastal Engineering (2013)
491 Final Report
492 [52] R.M. Larson, T.E. Hoerner, K.D. Smith, A.S. Wolters, Relationship between Skid Resistance
493 Numbers Measured with Ribbed and Smooth Tire and Wet Accident Locations, Final Report – State Job
494 Number 134323, 2008.
495 [53] F.G. Praticò, R. Vaiana
496 A study on the relationship between mean texture depth and mean profile depth of asphalt pavements
497 Constr. Build. Mater., 101 (2015), pp. 72-79, 10.1016/j.conbuildmat.2015.10.021
498 [54] M. Otsuki, H. Matsukawa, Systematic Breakdown of Amontons' Law of Friction for an Elastic
499 Object Locally Obeying Amontons' Law, Scientific Reports 3, Article number: 1586, 2013,
500 doi:http://dx.doi.org/10.1038/srep01586.
501 [55] A.J. Tuononen
502 Onset of frictional sliding of rubber-glass contact under dry and lubricated conditions

503 Sci. Rep., 6 (2016), p. 27951, 10.1038/srep27951
504 [56] K. Hallas, G. Hunwin, A study of pendulum slider dimensions for use on profiled surfaces, RR726
505 Research Report, Health and Safety Executive 2009, Health and Safety Laboratory, 2009.
506 [57] S.G. Kim, K.W. Kim
507 Influence of pad–pivot friction on tilting pad journal bearing
508 Tribol. Int., 41 (2008), pp. 694-703, 10.1016/j.triboint.2007.12.003
509 [58] G. Inturri, Cenni di meccanica della locomozione: aderenza e resistenza al moto, Corso di
510 Fondamenti di Trasporti, Corso di laurea Ingegneria Civile, Università di Catania, 2012.
511 [59] ASTM E 303
512 Standard Test for Measuring Surface Frictional Properties Using the British Pendulum Tester
513 (2008)